RAMAN MODE-SELECTIVE SPECTROSCOPIC IMAGING OF REDOX STATE IN FMN AND FLAVOPROTEIN

Min Gu

A Thesis

Submitted to the Graduate College of Bowling Green
State University in partial fulfillment of
the requirements for the degree of

MASTER OF SCIENCE

August 2014

Committee:

Hong Peter Lu, Advisor

Ksenija Glusac

Marshall Wilson

ABSTRACT

H. Peter Lu, Advisor

Incubated with silver nanoparticles coated with silica, we investigate the surface-enhanced Raman scattering (SERS) spectra of flavin monoucleotide (FMN) in different redox states. Good-quality spectra for oxidized and reduced FMN are obtained at different electrochemical potentials, respectively. Dominate Raman mode shifting occurring at 1623/1610, 1567/1550, 1502/1492 belonging to typical redox-sensitive region are observed and discussed, and they show a good consistency with calculations by using the DFT method. We assign the mode at 1500 cm^{-1}, composed of N_5-H bending, N_1=C_{10a} stretching and the asymmetric C_{4a}-N_5-C_{5a} stretching, as a spectroscopic indicator for the redox state of FMN, since it shows a significant downshift (1502/1492cm^{-1}) and non-linear correlation with potentials when FMN get reduced from the full oxidized state use the electrochemical method. Isolated FMN domain from wide type nNOS is studied with the same experimental approach and performs a similar Raman mode down-shifting as pure FMN, further supporting our conclusion that the mode at ~1500cm^{-1} indicates the redox states for FMN even in a protein environment.

To all my loves; to my lost youth; to a better me

ACKNOWLEDGMENTS

First, I would like to thank my father, my mother and my brother. They gave me solid support and courage to pursue my young dream in the US. Thanks to my uncle and aunt, who brought the family warmth here to me in this foreign country. Thank to my boyfriend Tao, who terminated my loneliness and offered me care and love. Without my family, I would not become who I am today.

I would like to extend my heartfelt gratitude to my advisor Dr. H. Peter Lu. His intelligence and patience encouraged me not only in my study but also in my life. His suggestions and advice guided me through all confusion and complexity to achieve the final goal. Thanks to him for his understanding in my personal choice. Thanks to my committee members Dr. Ksenija Glusac and Dr. R Marshall Wilson for serving in my committee by spending their valuable time. They gave me valuable advices and important encouragements.

I would like to thank to Dr. Yufan He, Dr. Desheng Zheng, Dr. Yuanmin Wang, Dr. Dibyendu Kumar Sasmal and Dr. Papatya Sevinc for their patient help and great advice during my master study. Furthermore, I would like to thank my group members Qian Wang, Maolin Lu, Zijian Wang, Qing Guo, Jin Cao and Bharat Dhital. It has been a wonderful time to work with them and study from them in Dr. Lu's group for the past three years.

I would like to thank Dr. Thomas H. Kinstle, Dr. Alexander N. Tarnovsky, Dr. Pavel Anzenbacher, Jr., Dr. Massimo Olivucci, Dr. R. Marshall Wilson and Dr. Andrew T. Torelli, who imparted advanced chemistry knowledge to me with their patience and professional skills. I would like to thank the faculty and the staff in the Department of Chemistry, especially Nora R Cassidy and Alita A Frater, for their generous help and support during my study time. Also, I would like to thank the ESOL instructors, especially Dr. Gary M Heba and Samuel Mac

Herrington for their precious advice and suggestions in improving my English writing and speaking. Thank to all my Chinese friends here in Bowling Green for sharing a wonderful time together with me. Finally, I am thankful to the Center for Photochemical Sciences and Bowling Green State University for giving me this great opportunity to study for the Chemistry Master.

TABLE OF CONTENTS

LIST OF FIGURES

LIST OF TABLES

INTRODUCTION

In the past over 30 years, surface enhanced Raman scattering (SERS) has been demonstrated to be a significantly powerful analytical technique for the sensitive and selective detection of molecules adsorbed on noble metal nanostructures. The use of SERS for the study biologically important molecules including heme-containing proteins[1], porphyrins[2], and highly organized systems such as photosynthetic reaction centers[3] and membrane preparations and photosynthetic bacteria[4], is now well established.

SERS has been employed to study biological processes for several advantages in electrochemical environments. First, the technique is uniquely high sensitive to molecules adsorbed to the metal nanoparticles. In the current study, we apply sliver nanoparticles coated with silica. The thin silica shells successfully avoid interaction between molecules and the metal surface without reducing the enhancement from metal nanostructures. Second, the metal nanostructures also cause quenching of the fluorescence background helping getting better Raman spectroscopy, which is particularly important for the flavin molecules whose fluorescence is very strong[5]. The fluorescence quenching advantage of SERS is appealing for the study of flavins and flavoproteins since initial attempts to obtain vibrational spectra of flavins using conventional Resonance Raman (RR) are unsuccessful because of interference from the intense free flavin emission at around 530nm[6]. Third, the Raman cross section for water is low, so that SERS can be used to study in aqueous solution[7]. Finally, SERS can provide detailed information about molecules at different redox states accompanying with electrochemical reactions.

Flavins are very versatile coenzymes and play central roles in many oxidation-reduction reactions in living cells. Owing to the isoalloxazine moiety, flavins, including flavin monoucleotide (FMN), flavin dinucleotide (FAD), and riboflavin can participate in both direct

two electron and step by step reactions, existing in three redox states: oxidized, semiquinone, and reduced states (Illustrated in Figure1A). The hydride transfer reaction occurring at N_5- and N_1-H consecutively and losing nitrogen lone pairs and conjugated π orbital can be probed in Raman spectroscopy. The Flavin Raman spectroscopy has been studied for almost thirty years since Copeland and co-workers first obtained high quality spectra of free flavins[8] and flavoproteins[9] with SERS on colloidal silver. Xu[10] and co-workers study in situ electrochemical SERS for the semiquinone radical using roughened sliver electrodes by controlling PH values of the buffer solution. Zheng[11] and co-workers first report Resonance Raman spectra of fully reduced flavin as well as quantum calculations. However, quantitative comparison mode study between oxidized and reduced flavin is still not clear.

In the present study, we exam the electron transfer process of flavin reduction-oxidation reaction with electrochemical potential control correlated with SERS. FMN molecules are kept at fully reduced or oxidized state by applying more negative or positive potential than the formal redox value with a home-made cell, providing real-time SERS at the same time. We also discuss the typically redox-sensitive region at 1500~1600cm^{-1} which shows a good consistency with calculated data using the DFT method. Furthermore, we suggest that the mode at ~1500cm^{-1} which is composed of N_5-H bending, N_1=C_{10a} stretching and the asymmetric C_{4a}-N_5-C_{5a} stretching act as a spectroscopic indicator redox states of FMN. This suggestion extends since similar behavior is observed in FMN domain isolated from wide-type Neuronal nitric oxide synthase (nNOS) using the same SERS correlated with electrochemical measurement.

EXPERIMENTAL METHODS

Materials and Sample Preparation

Flavin mononucleotide (FMN), AgNO3, sodium citrate, and sodium silicate were purchased from Sigma Aldrich and used as received. Isolated FMN domain from wide-type nNOS was a gift from Dr. D. J. Stuehr (Cleveland Clinic Foundation). Sliver nanoparticles (AgNP) were synthesized by a standard sodium citrate reduction method[12]. To generate ultra thin silica shells, the active sodium silicate solution was added into the sliver colloids[13]. The surface topography of synthesized nanoparticles characterized by STEM could be found in our previous work[14]. The average size of the AgNP @ SiO_2 is ~ 60nm as shown in the Figure 1 inset. FMN solution was diluted to 5×10^{-9} M with buffer solution (40mM EPPS, 10% glycerol, 150mM NaCl, PH=7.6) and incubated with sliver nanoparticles overnight before SERS measurement.

Surface-Enhanced Raman Measurements and Electrochemical Control

All SERS spectra were recorded by using the home-modified confocal Raman microscope[15] with 30s integration time. A continuous-wave (CW) 488nm argon ion laser was used to excite the sample at approximately 6 mw for SERS. The setups were carefully calibrated using mercury lamp and cyclohexane before Raman measurements with a resolution of $2cm^{-1}$. A CHI 600C electrochemical workstation was used for performing electrochemical control, equipped with the home-made cell[16] (working electrode: Indium tin oxide (ITO)/glass coverglass; counter electrode: platinum wire; reference electrode: sliver wire). Dry ~40 μL incubating solution containing FMN and sliver nanoparticles on the ITO surface, then a solution of 0.1M NaCl was used as supporting electrolyte in our homemade cell. Cyclic voltammetry was first performed before each Raman measurement. In order to keep the sample at the fully reduced or

oxidized state, a more negative or positive potential than the formal redox value was applied, respectively.

Density Functional Theory Calculations

To analyze the oxidized and reduced form of FMN, geometry optimization and Raman frequency calculations were performed by the density functional theory (DFT) method on B3LYP level with a basis set of 6-31G (d) using the Gaussian 09 package. According to a comprehensive evaluation of Scott and Radom[17], the obtained frequencies were scaled by a factor of 0.9614. Molecular orbitals were calculated with the same basis set and visualized with Jmol (Jmol: an open-source Java viewer for chemical structures in 3D. http://www.jmol.org/). All calculations were carried out on a vector processor (Ohio Supercomputer Center, Columbus).

RESULTS AND DISCUSSIONS

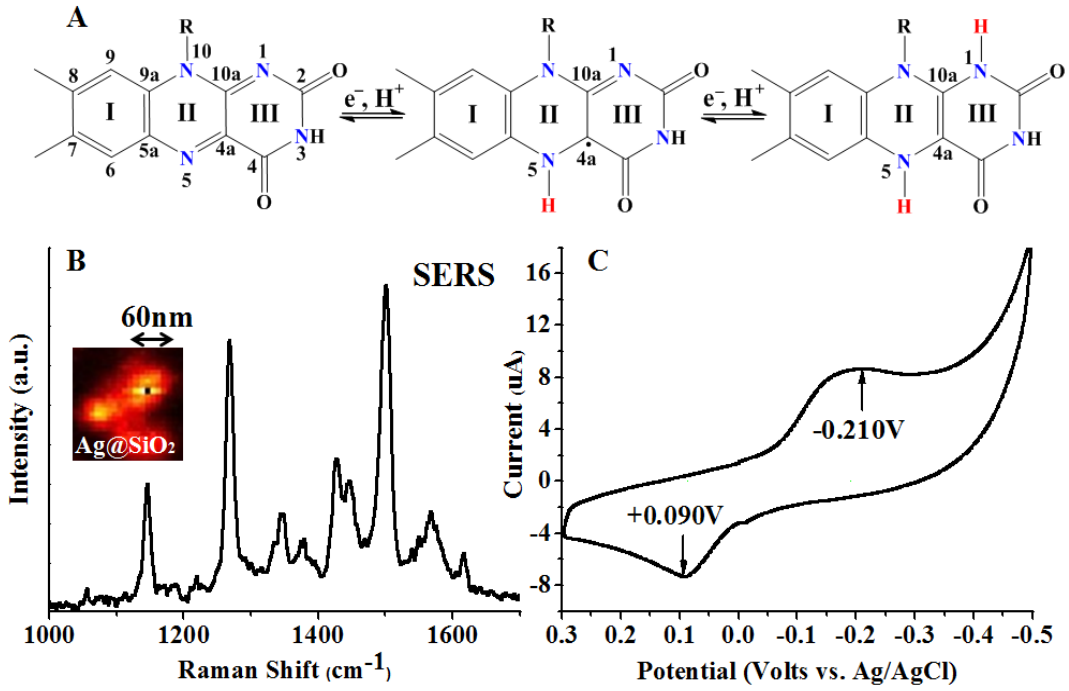

Figure 1. (A) Structure and numbering for the isoalloxazine ring of FMN and two-electron reduction processes. (B) A typical SERS spectrum of FMN incubated with AgNp@SiO2 at excitation frequency 448.16nm. A confocal image of a Raman-active dimer of AgNP@SiO2 is shown inset. (C) Cyclic voltammetric curve for FMN (5nM) with 0.1M NaCl solution adsorbed on the AgNP-coupled ITO surface. The Scan Rate = 0.1 v/s.

The gain or loss of an electron dramatically change the vibrational frequencies of the redox-sensitive bonds[6]. In flavin systems, the redox-sensitive bonds are readily identified as C_{4a}=N_5, C_{4a}-C_{10a}, and N_1=C_{10a} by structural comparison between the fully oxidized and reduced form in Figure 1A. Figure 1B shows the SERS spectrum of oxidized FMN adsorbed on sliver nanoparticles at +0.3V vs. Ag/AgCl when excited with 448nm argon ion laser light. The solution contains 10^{-9} M FMN and 0.1M NaCl at a PH value of 7.6 for which the electrochemical oxidation of FMN occurs at a potential around +0.090V and reduction potential at -0.210V as indicated by cyclic voltammetric curve shown in Figure 1C. The peak currents are proportional

to the square root of the sweep rate. At PH 7.6, the quite broad single peak is probably due to the mixing of the neutral and anion form of the redox species having different reduction potentials[10]. Compared to spectra reports in the literature, FMN exhibits the same SERS spectrum as Riboflavin, showing that (1) band positions and intensities are largely independent of the residue at N_{10}[18]; (2) the high quality SERS spectrum indicate a high fluorescence quenching efficiency with sliver nanoparticles in contrast to quenching with a protein or KI[19]; (3) electrochemical methods successfully control FMN to mainly stay at the fully oxidized state, using direct electron transfer between electrodes and molecules.

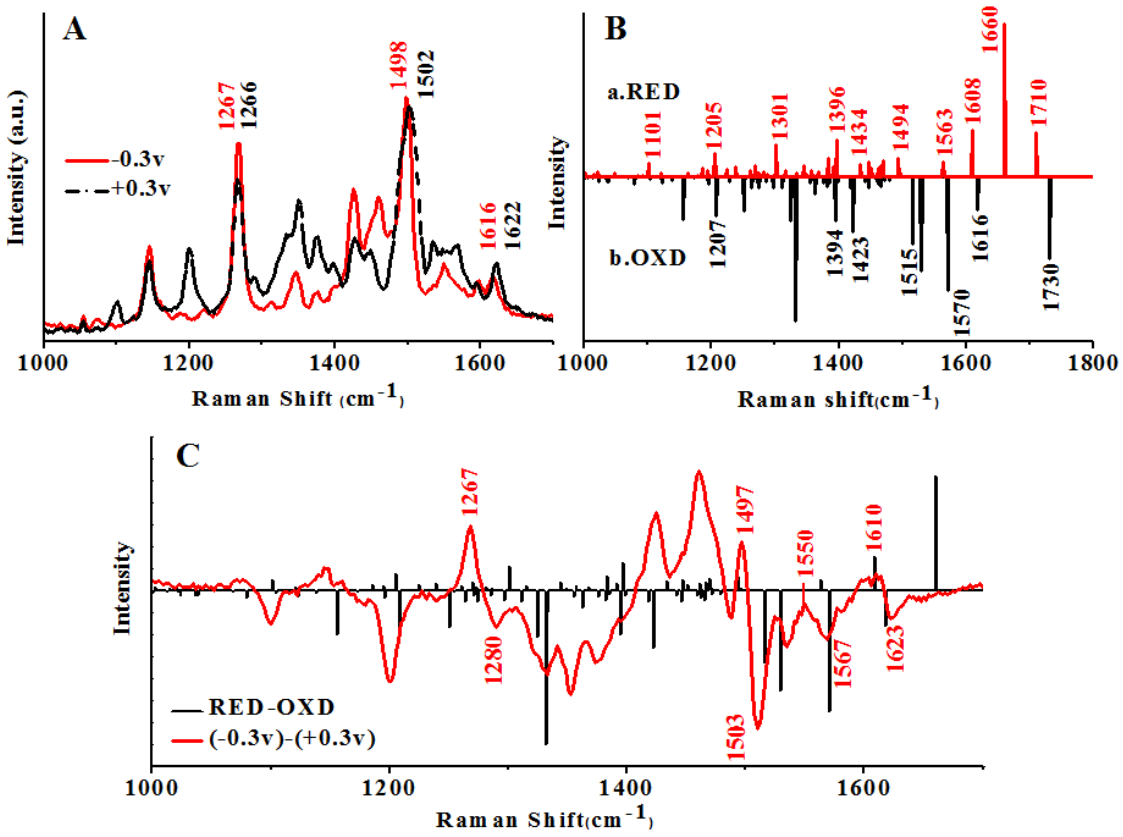

Figure 2. (A) SERS spectrum of FMN obtained at -0.3V and +0.3V vs. Ag/AgCl in PH 7.6 solution. (B) Calculated Raman frequency for FMN (Red: Reduced State, Black: Oxidized State), using DFT method by Gaussian 09 with B3LYP/6-31G (d) basis functions, scaling factor 0.9614. (C) Raman bands from subtraction (Red: Experiment data, Black: Calculated data).

Based on literature, the SERS spectra of FMN are characterized by a high-frequency region above 1000cm^{-1} with characteristic high-intensity modes, and a low-frequency, low-intensity region<1000cm^{-1}[118]. The latter contains in- and out- plane vibrations of the ribityl chain or the flavin ring system, which are not analyzed in this study. We first compare the fully oxidized with the fully reduced state of FMN, focusing on the 1700~1000cm^{-1} fingerprint region. We apply +0.3V to get the fully oxidized state and -0.3V to get the fully reduced state, since the oxidation potential is +0.090v and the reduced potential is -0.210v according to the CV curve. SERS spectra are recorded when potentials are on. Figure2A shows the SERS spectrum obtained at +0.3V (oxidized) and -0.3V (reduced) vs. Ag/AgCl. The electric stimulus produced direct electron transfer between the electrode and the target molecule, causing changes in SERS spectra correspondingly. In order to compare experimental data with theoretical data, we calculate Raman frequency for both reduced and oxidized FMN using the DFT method, the calculated data shown in Figure 2B. To isolate the shifting bands due to the state changing, a spectrum is obtained by subtracting the oxidized state (+0.3V) from the reduced state (-0.3V), shown in Figure 2C. Black vertical lines are calculated Raman frequency by doing the same subtraction with calculated data in Figure 2B. Comparing the experimental and the calculated data, they show a good consistence and the dominate peaks shifting occur at 1623/1610, 1567/1550, 1502/1492, 1310/1280 and 1267/1267cm^{-1}.

Table 1. Assignments of Important Raman Bands of FMN in Reduced and Oxidized States

Raman Bands(cm^{-1})		Approximate Descriptions
Reduced	Oxidized	
1267(1261)	1267(1264)	N_1-H, N_5-H, C_6-H, C_9-H,C_2=O
1279(1268)	1280(1274)	N_5-H, N_3-H, C_4=O
1497(1493)	1503(1517)	N_5-H, νN_5-C_{4a}, νN_1=C_{10a}, Ring I stretch
1550(1563)	1567(1571)	N_5-H, C_6-H, C_9-H, νN_1-C_{10a}-C_{4a}-N_5
1610(1609)	1623(1617)	νN_1=C_{10a}, C_2=O

Raman Frequencies shown in parentheses are calculated using density functional theory (DFT) by Gaussian 09 with B3LYP/6-31G (d) basis functions and scaled by a factor of 0.9614.

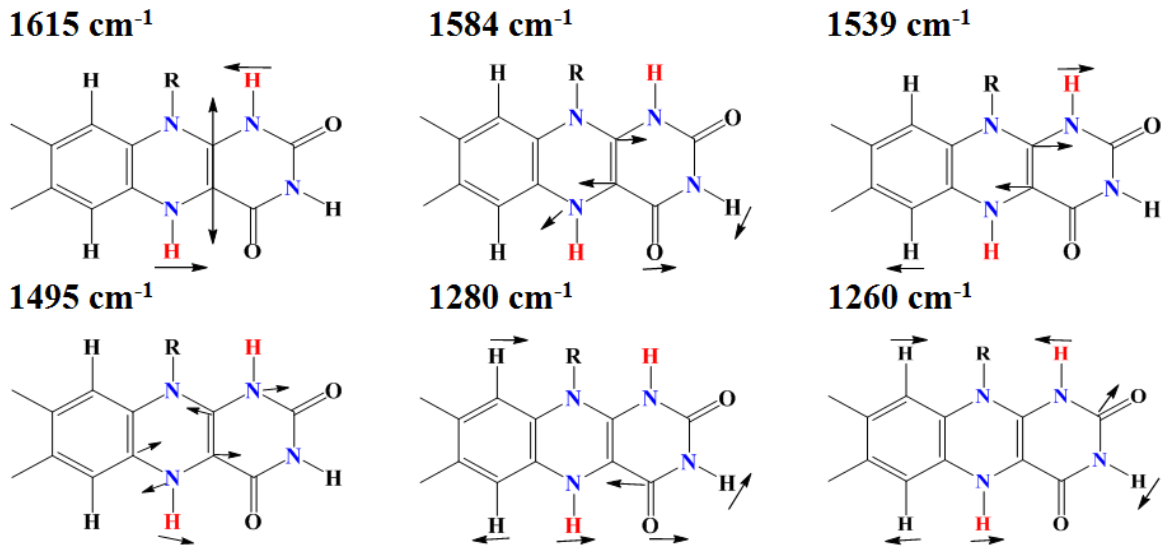

Figure 3. Normal modes of Raman bands for fully reduced FMN (only show isoalloxazine moiety).

Earlier studies using isotopic substitution and semi-empirical calculation provided assignment of both fully oxidized[20] and fully reduced isoalloxazine ring[11, 21]. On the basis of literature and calculations[22], our approximate description of the Raman bands are given in Table 1 and a diagram describing the normal modes of fully reduced flavin is given in Figure 3.

The band shift from 1623 to 1610cm^{-1} involves the significant contribution from a combination of C_2=O and C_{10a}=N_1 stretching motion[23]. Protonation at the N_5 and N_1 position changed the double bond between C_{10a} and N_1 to single bond, altering the conjugated pathway in C_{10a}=N_1-C_2=O consistent with a decrease in frequency. Having large isotope shifts for $^{15}N_5$ and $^{13}C_{4a}$, the 1584 cm^{-1}band is well known to have a major component of the N_5=C_{4a}-C_{10a}=N_1 conjugation pathway. Dutta and Spiro demonstrated that the 1584 and 1611 cm^{-1} modes of oxidized flavin and semiquinone are the only bands that are observed to be enhanced in the second π-π* transition of these two species[24]. It appears that the molecular distortion in the second π-π* transition specially involves a large displacement along the 1584cm^{-1} mode. It also involves a significant contribution of C_{10a}=N_1 stretching. In other words, it strongly involves the N_5=C_{4a}-C_{10a}=N_1 conjugation pathway, accounting for the large downshift of band at 1584cm^{-1} when the conjugation pathway is altered by substitution at position 8[23, 25]. The 1548cm^{-1} band also involves C_{4a}=N_5 and C_{10a}=N_1stretching. H bonding to either N_5 or N_1 is expected to lower the band frequency as these heteroatoms are at either end of the conjugated double system. Mode at 1539cm^{-1} is mainly composed of the N_1-C_{10a} stretching and ring I symmetric modes[23] and is expected to get strong resonance Raman enhancement due to a large change in polarizability along those symmetric modes. It shows a great downshift from 1594cm^{-1} to 1550cm^{-1} in our data consistent with the assignment.

The mode at 1498cm^{-1} is mainly composed of N_5-H bending, to which N_1=C_{10a} stretching and the asymmetric C_{4a}-N_5-C_{5a} stretching are coupled[26]. Hydrogen bonding definitely alters the electronic structure as predicted by the theoretical calculations[27] and substantiated by the ^{13}C-NMR observations[28]. Protonation at N_5 slightly weakens C_{4a}-N_5 and then protonation at N_1

weakens N_1=C_{10a}, inducing the downshift from 1502 to 1492cm^{-1}. Detailed Raman shifting correlated to potential changing will be discussed later.

Comparison of our SERS spectra recorded at more negative than -0.3v with the fully reduced flavin and semiquinone form of flavin from the literature shows that we obtain the fully reduced form. Mode at 1500cm^{-1}~1600cm^{-1} is typically the redox-sensitive region. Earlier Raman spectroscopic analysis indicates that the 1625, 1550, and 1500cm^{-1} bands are associated mainly with stretching vibration of the isoalloxazine ring I and /or stretching vibration of the C_{10a}-N_1 and N_5-C_{4a} that are coupled to the ring I mode.

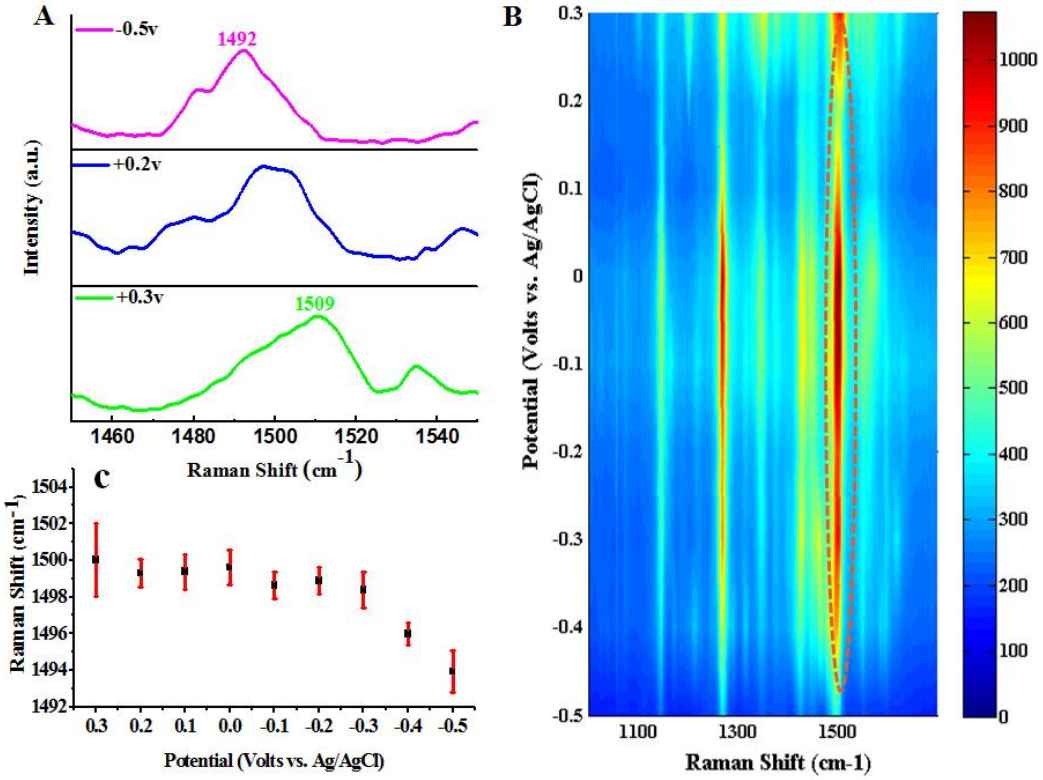

Figure 4. (A) Three different averaged SERS spectrum obtained at -0.5v, +0.2v and +0.3v, respectively. (B) Voltage-dependent SERS spectrum with the mode at 1495 cm^{-1} highlighted. (C) The downshift of mode at 1495cm^{-1} when the potential changes from +0.3V to -0.5 V.

Comparing the 1500cm^{-1} band corresponding to the potential, it is clear that it gradually shifts from 1502cm^{-1} to 1492cm^{-1}. Each spectrum shown in Figure 4A is the average value from 10 spectra under their specific potential. Three spectra are shown as a zoom-in view of a spectral fluctuation trajectory (Figure 4B) to illuminate the spectra fluctuation evolution profile of redox-sensitive mode at~1500cm^{-1} associating with C_{10a}-N_1[25-26]. In Figure 4C, we continuously apply potential from +0.3V to -0.5V and record the Raman frequency for mode at~1500 from 25 spectra for each potential. The band is not linearly downshifting but shows some fluctuation because: (1) the experiment is not under single-molecule level as our previous work; Raman frequency here are showing the dominate states for multiple molecules; (2) At PH=7.6, cation or anion may both occur in solution and the flavin may have semiquinone form and broaden the Raman peak; (3) Delocalization of electrons at the highly conjugated region N_5-C_{4a}-C_{10a}-N_1 as described above cause fluctuation of the spectra. Comparing calculated HOMO orbitals for FMN and $FMNH_2$ shown in Figure 5, we observe that the electron density changes dramatically in N_5-C_{4a}-C_{10a}-N_1. Besides, we notice that the 1500cm^{-1} band shows slightly up-shifting when potential changes from -0.1V to -0.2V, indicating that N_1=C_{10a} becomes stronger once N_5 gets protonation, and after that it performs down-shifting because the molecule becomes fully reduced and turns to be much weaker on N_1 protonation. Furthermore, bands at 1500, 1410, and 1355cm^{-1} are also empirical markers on the flavin ring in different dielectric environment[25].

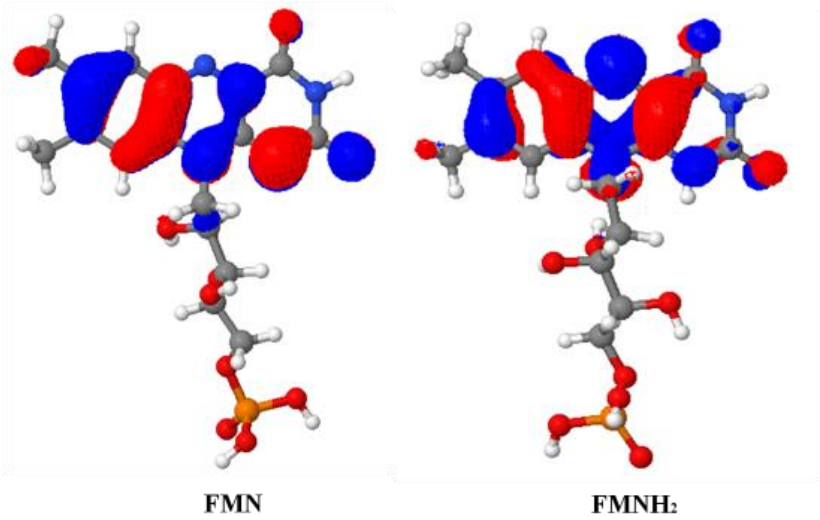

Figure 5. Calculated HOMO orbitals for FMN and FMNH2, visualized with Jmol (Jmol: an open-source Java viewer for chemical structures in 3D. http://www.jmol.org/)

Surface Enhanced Raman Spectra of FMN domain from nNOS

Nitric oxide synthases (NOSs) are now well-known enzymes for producing NO, which is identified as an essential regulator in mammalian biology. Containing two monomers associated with two calmodulins (CaM), they are tetramers including FAD, FMN, iron protoprphyrin (heam) and cofactors (6R)-5, 6, 7, 8-tetrahydrobioprotein (BH_4)[29]. Based on different genes' products, locations, catalytic properties and inhibitor sensitivity, NOS have three mammalian isoforms: neuronal, endothelial and inducible NOS (nNOS, eNOS and iNOS, respectively). Activated by calmodulin (CaM), NO is synthesized by NOS in a reaction of L-arginine, NADPH and oxygen to citrulline and NADP[30], where the conformation of the FMN domain changes from its shielded electron-accepting state to a new electron-donating state[31]. In the two states, the FMN domain is engaged in distinctly different interdomain interactions and the module swings back and forth to contact the $NADP^+$-FAD reductase module and the NOS heme domain[32]. However, the mechanisms by which the FMN domain functions in the NOS catalysis and the electron transfer are coupled to substrate oxidation are unclear and remain a major challenge in current NOS

study[33]. In this work, we probe the redox states of FMN molecule in FMN domain/CaM complex isolated from wide-type nNOS by a combined SERS spectroscopy and electrochemical control approach. Since there are still no available crystal structures for isolated nNOS-FMN domain, we adopt a human iNOS-FMN domain to illustrate the basic structure information shown in Figure 6.

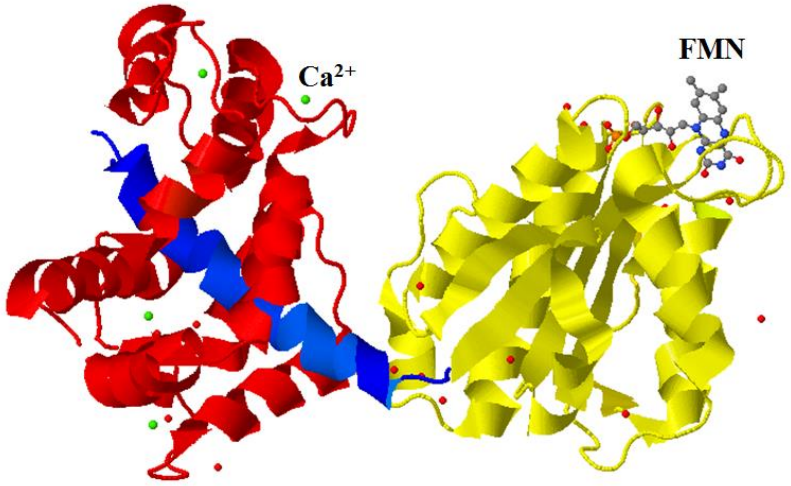

Figure 6. Crystal structure of a human iNOS FMN domain/CaM complex (PDB 3HR4). The FMN domain is yellow, and the CaM-binding linker between the FMN and heme domains is blue. The CaM molecule is red, and Ca^{2+} ions are green spheres.

We prepare the nNOS-FMN domain sample with the same buffer solution and same method as described above. After applying cyclic voltammetryshown in Figure 7A, we get reduction potential (-0.236v) and oxidation potential (+0.072v), and they are very close to values obtained with pure FMN molecules (reduced: -0.210v, oxidized: +0.090v, respectively), revealing a good electronic communication between FMN domain and the electrode. In Figure 7B, comparing SERS spectra obtained at the fully reduced (-0.5v) and the oxidized (+0.5v) state, we observed dominant peaks shifting at1550/1535cm^{-1}, 1501/1496, which belong to the typical redox-sensitive region. 1550cm^{-1} is mainly composed of the N_1-C_{10a} stretching and ring I symmetric modes[23], and it is expected to get strong resonance Raman enhancement due to a large

change in polarizability along those symmetric modes. 1500cm^{-1} contains N_5-H bending, coupled with N_1=C_{10a} stretching and the asymmetric C_{4a}-N_5-C_{5a} stretching. Protonation at N5 slightly weakens C_{4a}-N_5 and then protonation at N_1 weakens N_1=C_{10a}, inducing the downshift. Plotting the Raman band position averaged from 25 successive spectra at ~1500cm^{-1} in Figure 7C, it showing similar downshift when potential change from +0.3v to 0.5v, consistent with our conclusion that downshifting at ~1500cm^{-1} indicates redox states of FMN even in the protein environment. Also, we notice that the 1500cm^{-1} band shows slight upshifting when potential changes from +0.1V to 0V, indicating that N_1=C_{10a} becomes stronger once N_5 gets protonation, and after that it performs down-shifting because the molecule becomes fully reduced and becomes much weaker on N_1 protonation.

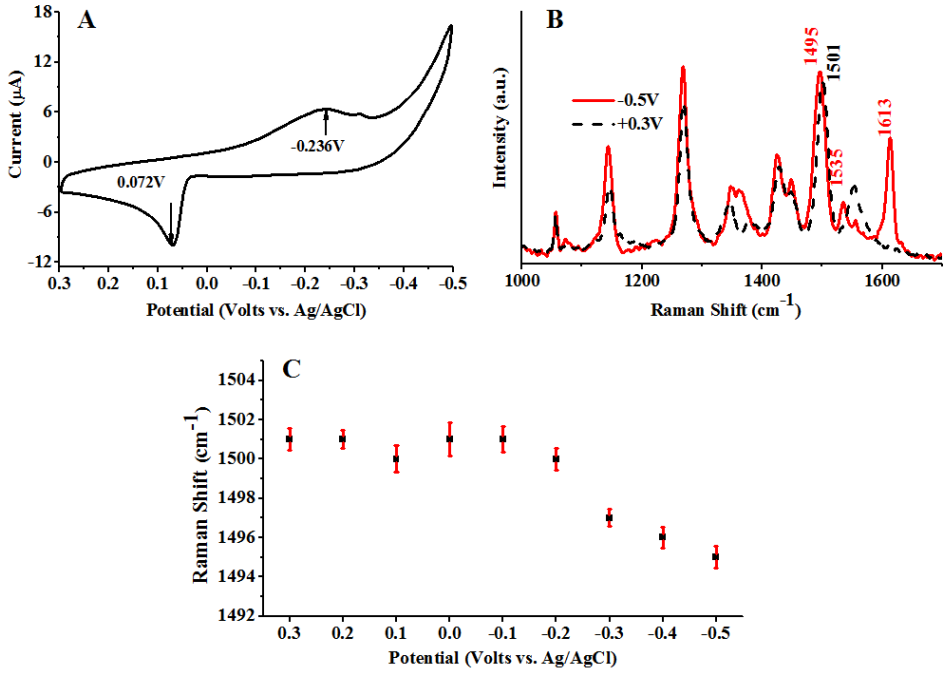

Figure 7. (A) Cyclic voltammetric curve for the nNOS FMN domain/CaM complex (5nM) with 0.1M NaCl. The Scan Rate = 0.1 v/s. (B) SERS spectrum for the nNOS FMN domain/CaM complex from the experiment at +0.3v and -0.5V, respectively. (C) The downshift of the mode at 1495cm^{-1} when the potential changes from +0.3V to -0.5 V.

CONCLUSIONS

To study the electron transfer process of flavin reduction-oxidation reaction, we apply a electrochemically potential control method correlated with surface enhanced Raman scattering. Our results reveal that FMN molecules are efficiently kept at reduced or oxidized state at specific potentials and provide real-time SERS imaging. We have observed and discussed dominate peak shifting occurring at 1623/1610, 1567/1550 and 1502/1492 cm^{-1}, belonging to the typical redox-sensitive region according to the literature, which are all assigned to the electron transfer reaction parts in the isoalloxazine ring. Our experimental Raman modes show a good consistency with calculated data using DFT method. Different from traditional redox state marker mode~1584 cm^{-1}, we suggest that the Raman mode at ~1500cm^{-1} acts as an indicator of redox states for FMN, since it shows significant downshift from ~1502cm^{-1} to 1492cm^{-1} and non-linear correction with potentials when FMN gets reduced from oxidized states electrochemically, even in isolated NOS domain containing FMN.

REFERENCES

1. Hildebrandt, P.; Stockburger, M., Surface-Enhanced Resonance Raman-Spectroscopy of Cytochrome-C at Room and Low-Temperatures. *J Phys Chem-Us* **1986,** *90* (22), 6017-6024.

2. Cotton, T. M.; Schultz, S. G.; Vanduyne, R. P., Surface-Enhanced Resonance Raman-Scattering from Water-Soluble Porphyrins Adsorbed on a Silver Electrode. *Journal of the American Chemical Society* **1982,** *104* (24), 6528-6532.

3. Cotton, T. M.; Vanduyne, R. P., Resonance Raman-Scattering from Rhodopseudomonas-Sphaeroides Reaction Centers Absorbed on a Silver Electrode. *Febs Lett* **1982,** *147* (1), 81-84.

4. (a) Babij, R.; Lee, M.; Cortes, E.; Vonsattel, J. P.; Faust, P. L.; Louis, E. D., Purkinje cell axonal anatomy: quantifying morphometric changes in essential tremor versus control brains. *Brain : a journal of neurology* **2013,** *136* (Pt 10), 3051-61; (b) Picorel, R.; Holt, R. E.; Cotton, T. M.; Seibert, M., Surface-enhanced resonance Raman scattering spectroscopy of bacterial photosynthetic membranes. The carotenoid of Rhodospirillum rubrum. *The Journal of biological chemistry* **1988,** *263* (9), 4374-80.

5. Dutta, P. K.; Nestor, J. R.; Spiro, T. G., Resonance Coherent Anti-Stokes Raman-Scattering Spectra of Fluorescent Biological Chromophores - Vibrational Evidence for Hydrogen-Bonding of Flavin to Glucose Oxidase and for Rapid Solvent Exchange. *Proceedings of the National Academy of Sciences of the United States of America* **1977,** *74* (10), 4146-4149.

6. Holt, R. E.; Cotton, T. M., Surface-Enhanced Resonance Raman and Electrochemical Investigation of Glucose-Oxidase Catalysis at a Silver Electrode. *Journal of the American Chemical Society* **1989,** *111* (8), 2815-2821.

7. Abdelsalam, M.; Bartlett, P. N.; Russell, A. E.; Baumberg, J. J.; Calvo, E. J.; Tognalli, N. G.; Fainstein, A., Quantitative electrochemical SERS of flavin at a structured silver surface. *Langmuir* **2008,** *24* (13), 7018-7023.

8. Copeland, R. A.; Fodor, S. P. A.; Spiro, T. G., Surface-Enhanced Raman-Spectra of an Active Flavo Enzyme - Glucose-Oxidase and Riboflavin Binding-Protein on Silver Particles. *Journal of the American Chemical Society* **1984,** *106* (13), 3872-3874.

9. Copeland, R. A.; Spiro, T. G., Ultraviolet Resonance Raman-Spectroscopy of Flavin Mononucleotide and Flavin Adenine-Dinucleotide. *J Phys Chem-Us* **1986,** *90* (25), 6648-6654.

10. Xu, J.; Birke, R. L.; Lombardi, J. R., Surface-Enhanced Raman-Spectroscopy from Flavins Adsorbed on a Silver Electrode - Observation of the Unstable Semiquinone Intermediate. *Journal of the American Chemical Society* **1987,** *109* (19), 5645-5649.

11. Zheng, Y. G.; Carey, P. R.; Palfey, B. A., Raman spectrum of fully reduced flavin. *J Raman Spectrosc* **2004,** *35* (7), 521-524.

12. Lee, P. C.; Meisel, D., Adsorption and Surface-Enhanced Raman of Dyes on Silver and Gold Sols. *J Phys Chem-Us* **1982,** *86* (17), 3391-3395.

13. Liz-Marzan, L. M.; Giersig, M.; Mulvaney, P., Synthesis of nanosized gold-silica core-shell particles. *Langmuir* **1996,** *12* (18), 4329-4335.

14. Wang, Q.; Wang, Y. M.; Lu, H. P., Revealing the secondary structural changes of amyloid beta peptide by probing the spectral fingerprint characters. *J Raman Spectrosc* **2013,** *44* (5), 670-674.

15. Lu, H. P., Site-specific Raman spectroscopy and chemical dynamics of nanoscale interstitial systems. *J Phys-Condens Mat* **2005,** *17* (7), R333-R355.

16. Wang, Y. M.; Sevinc, P. C.; He, Y. F.; Lu, H. P., Probing Ground-State Single-Electron Self-Exchange across a Molecule-Metal Interface. *Journal of the American Chemical Society* **2011,** *133* (18), 6989-6996.

17. Scott, A. P.; Radom, L., Harmonic vibrational frequencies: An evaluation of Hartree-Fock, Moller-Plesset, quadratic configuration interaction, density functional theory, and semiempirical scale factors. *J Phys Chem-Us* **1996,** *100* (41), 16502-16513.

18. Su, Y.; Tripathi, G. N. R., Time-Resolved Resonance Raman Observation of Protein-Free Riboflavin Semiquinone Radicals. *Journal of the American Chemical Society* **1994,** *116* (10), 4405-4407.

19. (a) Lee, N. S.; Sheng, R. S.; Morris, M. D.; Schopfer, L. M., The Active Species in Surface-Enhanced Raman-Scattering of Flavins on Silver Colloids. *Journal of the American Chemical Society* **1986,** *108* (20), 6179-6183; (b) Lee, N. S.; Hsieh, Y. Z.; Morris, M. D.; Schopfer, L. M., Reinterpretation of Surface-Enhanced Resonance Raman-Scattering of Flavoproteins on Silver Colloids. *Journal of the American Chemical Society* **1987,** *109* (5), 1358-1363; (c) Holt, R. E.; Cotton, T. M., Free Flavin Interference in Surface Enhanced Resonance Raman-Spectroscopy of Glucose-Oxidase. *Journal of the American Chemical Society* **1987,** *109* (6), 1841-1845.

20. Benecky, M.; Yu, T. Y.; Watters, K. L.; Mcfarland, J. T., Metal-Flavin Complexation - a Resonance Raman Investigation. *Biochimica et biophysica acta* **1980,** *626* (1), 197-207.

21. Nishina, Y.; Sato, K.; Miura, R.; Matsui, K.; Shiga, K., Resonance Raman study on reduced flavin in purple intermediate of flavoenzyme: use of [4-carbonyl-18O]-enriched flavin. *Journal of biochemistry* **1998,** *124* (1), 200-8.

22. Lively, C. R.; Mcfarland, J. T., Assignment and the Effect of Hydrogen-Bonding on the Vibrational Normal-Modes of Flavins and Flavoproteins. *J Phys Chem-Us* **1990,** *94* (10), 3980-3994.

23. Bowman, W. D.; Spiro, T. G., Normal Mode Analysis of Lumiflavin and Interpretation of Resonance Raman-Spectra of Flavoproteins. *Biochemistry* **1981,** *20* (11), 3313-3318.

24. Dutta, P. K.; Spiro, T. G., Resonance Coherent Anti-Stokes Raman-Scattering Spectra of Oxidized and Semi-Quinone Forms of Clostridium Mp Flavodoxin. *Biochemistry* **1980,** *19* (8), 1590-1593.

25. Zheng, Y.; Dong, J.; Palfey, B. A.; Carey, P. R., Using Raman spectroscopy to monitor the solvent-exposed and "buried" forms of flavin in p-hydroxybenzoate hydroxylase. *Biochemistry* **1999,** *38* (51), 16727-32.

26. Li, J.; Uchida, T.; Ohta, T.; Todo, T.; Kitagawa, T., Characteristic structure and environment in FAD cofactor of (6-4) photolyase along function revealed by resonance Raman spectroscopy. *The journal of physical chemistry. B* **2006,** *110* (33), 16724-32.

27. Nishimoto, K.; Watanabe, Y.; Yagi, K., Hydrogen bonding of flavoprotein. I. Effect of hydrogen bonding on electronic spectra of flavoprotein. *Biochimica et biophysica acta* **1978,** *526* (1), 34-41.

28. Muller, F.; Grande, H. J.; Harding, L. J.; Dunham, W. R.; Visser, A. J.; Reinders, J. H.; Hemmerich, P.; Ehrenberg, A., On the molecular and submolecular structure of the semiquinone cations of alloxazines and isoalloxazines as revealed by electron-paramagnetic-resonance spectroscopy. *European journal of biochemistry / FEBS* **1981,** *116* (1), 17-25.

29. Crane, B. R.; Arvai, A. S.; Gachhui, R.; Wu, C. Q.; Ghosh, D. K.; Getzoff, E. D.; Stuehr, D. J.; Tainer, J. A., The structure of nitric oxide synthase oxygenase domain and inhibitor complexes. *Science* **1997,** *278* (5337), 425-431.

30. (a) Knowles, R. G.; Moncada, S., Nitric-Oxide Synthases in Mammals. *Biochem J* **1994,** *298*, 249-258; (b) Xie, Q. W.; Nathan, C., The High-Output Nitric-Oxide Pathway - Role and Regulation. *J Leukocyte Biol* **1994,** *56* (5), 576-582.

31. Adak, S.; Sharma, M.; Meade, A. L.; Stuehr, D. J., A conserved flavin-shielding residue regulates NO synthase electron transfer and nicotinamide coenzyme specificity. *Proceedings of the National Academy of Sciences of the United States of America* **2002,** *99* (21), 13516-13521.

32. (a) Stuehr, D. J.; Tejero, J.; Haque, M. M., Structural and mechanistic aspects of flavoproteins: electron transfer through the nitric oxide synthase flavoprotein domain. *Febs J* **2009,** *276* (15), 3959-3974; (b) Haque, M. M.; Panda, K.; Tejero, J.; Aulak, K. S.; Fadlalla, M. A.; Mustovich, A. T.; Stuehr, D. J., A connecting hinge represses the activity of endothelial nitric oxide synthase. *Proceedings of the National Academy of Sciences of the United States of America* **2007,** *104* (22), 9254-9259; (c) Stuehr, D. J.; Tejero, J.; Haque, M. M., Structural and mechanistic aspects of flavoproteins: electron transfer through the nitric oxide synthase flavoprotein domain. *Febs J* **2009,** *276* (15), 3959-74.

33. Feng, C. J., Mechanism of nitric oxide synthase regulation: Electron transfer and interdomain interactions. *Coordin Chem Rev* **2012,** *256* (3-4), 393-411.